Reviewers 3

General comment: The manuscript proposes the use of a novel polymer to enhance the oil recovery.

Discussion: We sincerely appreciate this reviewer for the encouraging comments, recommendations, and detailed suggestions regarding the improvement of our manuscript, and we carefully addressed his/her questions as follows.

Issue 1: The last part of the introduction from "in this study" to the end sounds as a summary and it does not state which is the aim and the novelty of the work. This part must be shortened and revised.

Discussion: We appreciate this comment. We have modified the last paragraph of the introduction to explain the purpose and novelty of this work. The results of the modification are as follows.

In this study, based on the cost-effectiveness of materials and the difficulty of synthesis, we selected acrylamide and 2-acrylamido-2-methylpropane sulfonic acid commonly used in oil fields as hydrophilic monomers, and selected long-chain lauryl acrylate and benzyl acrylate with benzene ring as hydrophobic monomers to prepare amphiphilic polymers PAALB through free radical polymerization. The addition of acrylamide and 2-acrylamido-2-methylpropanesulfonic acid effectively improved the viscosity, temperature resistance and salt resistance of the polymer solution. The addition of monomers with long chains provided the polymers with interfacial activity. The addition of monomers containing benzene rings facilitates the dispersion of heavy oil components in the polymer, thus enhancing the interaction between the polymer and the heavy oil. The amphiphilic polymer has excellent interfacial activity, emulsifying ability and viscoelasticity, which can both reduce the viscosity of the oil phase and increase the viscosity of the aqueous phase. This enhancement changes the water-oil mobility ratio, increases sweep volumes, and contributes to the overall enhancement of heavy oil recovery. In addition, an important capability of our synthesized amphiphilic polymers is the ability to achieve self-emulsification of heavy oil. However, in the reports on spontaneous emulsification of crude oil, the viscosity of most crude oil is lower than 5000 mPa·s, and the spontaneous emulsification of heavy oil above 10000 mPa·s is not reported. Therefore, this amphiphilic polymer has better applicability to the self-emulsification and viscosity reduction of high viscosity heavy oils.

Issue 2: How were determined the data reported in Table 1 and Table 2?

Discussion: We apologize for the lack of experimental methods. The test results of heavy oil properties in Table 1 are provided by China State Key Laboratory of Heavy Oil. The test methods used are as follows: The relative density data were obtained according to the Chinese standard 《GB/T2540-1981 Petroleum Product density determination method (Specific gravity bottle method)》. Heavy oil viscosity data were obtained using a HAAKE MARS III rheometer. In viscosity tests, the CC24Ti tumbler measuring system is selected for system viscosity determination, the test mode is CR, the shear speed is 7.34 s^{-1}, the time is 300 s, the measurement point is 30, the temperature is 50 °C. The content data of components of heavy oil were obtained according to the method in Chinese standard 《NB/SH/T 0509-2010 Determination of four components of Petroleum Asphalt》. The data of heavy oil wax content were obtained according to the method in Chinese standard 《SH/T 0778-2005 Method for determination of petroleum asphalt wax content》. Test results for the component content of the brine water in Table 2 were provided by Pony Testing Company. The contents of Cl^- and SO_4^{2-} were determined by ion chromatography, Na^+, K^+, Ca^{2+} and Mg^{2+} by inductively coupled plasma emission spectrometry, and HCO_3^- by potentiometric titration.

Issue 3: Paragraph 2.2 How was controlled the polymerization of the polymer? How the different monomers can react to give the reported polymer architecture? The rationale about the synthesis must be better explained. The information on the molecular weight of the polymer must be provided as well as the monomer ratio. The amphiphilicity of the polymer must be better explained.

Discussion: We appreciate this comment. First, regarding the synthesis principle, we synthesized the reported polymers by free radical polymerization. In the reaction, the monomers are olefinic monomers, and the addition polymerization reaction occurs through the double-healthy opening (as shown in Fig. 1). This polymerization reaction usually consists of three elementary reactions: chain initiation, chain growth, and chain termination. In the chain initiation stage, the initiator we add decomposes under the effect of heat to produce primary radicals (as in Figure 2), and the primary radicals add to the monomers to produce monomer radicals (as in Figure 3). In the chain growth stage, the monomer radical continues to open other π-bonded monomers to form new chain radicals, and so on (as in Figure 4). This stage of the reaction is exothermic, the activation energy is low, the reaction rate is extremely high, and the degree of polymerization reaches thousands to tens of thousands in a few seconds, so there are often only monomers and polymers within the free radical polymerization reaction system, and a series of

intermediates with increasing degrees of polymerization do not exist. At the chain termination stage, the chain radicals become inactive and a stable polymer is formed (e.g., Figure 5). Usually when the monomers have been consumed and the reaction is nearing its end.

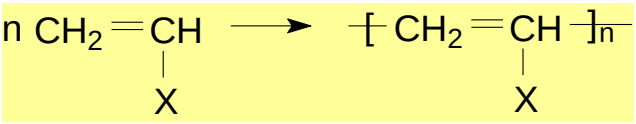


Figure 1. Olefin monomers undergo addition polymerization

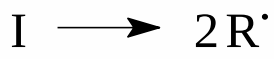


Figure 2. Primary free radicals are generated from the decomposition of initiators



Figure 3. Addition of primary radicals to monomers produces monomer radicals

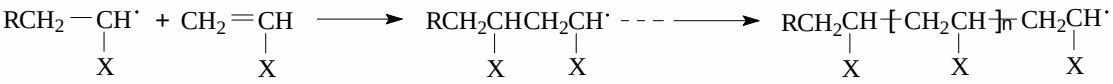


Figure 4. Chain growth stage



Figure 5. Chain termination stage

Secondly, we added elemental analysis and molecular weight distribution characterization tests of copolymers. The test results are as follows.

Test method:

C, H, O, N, and S quantities were determined using the Vario EL cube and Vario MACRO cube elemental analyzer.

Gel permeation chromatography (GPC) was performed using an Agilent 1260 Infinity II LC liquid chromatograph equipped with an Agilent RID G1362A detector on a Waters Ultrahydrogel 300 x 7.8mm 500-250-120A column. 0.1 mol/L NaNO3 aqueous solution was used as the mobile phase at a flow rate of 1mL/min. The testing temperature was 40℃, and the polymer sample concentration was 5000 mg/L.

Results and Discussions:

1. Elemental analysis

The results from the elemental analysis of the polymer are shown in Table 1. According to theoretical calculation, when the molar ratio of AM:AMPS:LA:BA is 6:2:1:1, the mass proportion of

each element in the polymer is C (55.07%), H (7.57%), O (23.19%), N (9.02%) and S (5.15%), respectively. Although there is some deviation between the test results of element analysis and the theoretical calculation results, the overall results are similar, and the deviation is very slight. The test results show that the monomer composition of the polymer is consistent with the feed ratio.

Table 1. Elemental analysis results of the PAALB

Element	C	H	O	N	S
Theoretical content (wt %)	55.07	7.57	23.19	9.02	5.15
Measurement content (wt %)	50.77	7.41	28.54	8.35	5.02

We have attached the data from the elemental analysis test results of the polymer, in which we named the sample of polymer PAALB as "231101091146-LB-1", as shown in Figure 6 below.

Document:Untitled(vario EL cube) from:--.--.--(modified)

Analytic functional testing
Vario EL cube
Serial number:19103023
Text report

Weight(mg)	Name	C[%]	N[%]	H[%]	S[%]
6.0520	Sulfanilamide	41.81	16.25	4.650	18.620
9.3840	231101091146-B-1	47.99	8.49	7.865	5.047
10.9540	231101091146-LB-1	50.77	8.35	7.410	5.023

Document:Untitled(vario EL cube) from:--.--.--(modified)

Analytic functional testing
Vario EL cube
Serial number: 19103023

Text report

Weight(mg)	Name	O[%]
4.9960	benzoic acid	26.200
6.4470	231101091146-B-1	30.227
8.1205	231101091146-LB-1	28.542

Figure 6. Elemental analysis data for the polymer PAALB

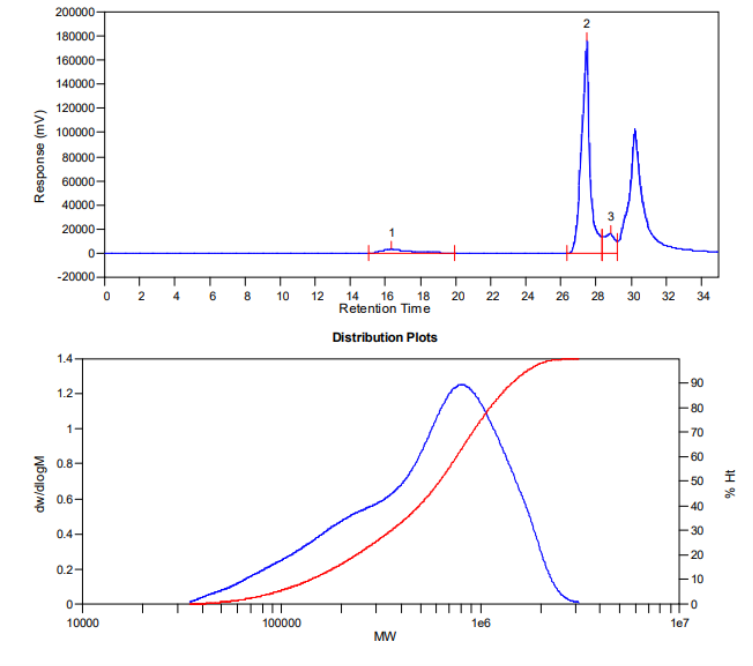
2. Relative molecular mass of polymers and its distribution

Table 2 shows the relative molecular mass distribution of polymer PAALB. As can be seen from Table 2, the number average relative molecular mass (M_n) of the polymer is 307883, the weight average relative molecular mass (M_w) is 679306, the Z average relative molecular mass (M_z) is 1048818, the Z+1 average relative molecular mass (M_{z+1}) is 1333611, and the viscosity average relative molecular mass (M_v) is 623887. The polymer's relative molecular mass polydispersity index (PDI) was 2.21, and the test results proved the successful preparation of the polymer.

Table 2. Gel permeation chromatography results of PAALB

M_n	M_w	M_z	M_{z+1}	M_v	PDI
307883	679306	1048818	1333611	623887	2.21

We have attached the gel permeation chromatography test data for the polymer as shown in Figure 7 below.



Narrow Standard Report

Peak No	Mp	Mn	Mw	Mz	Mz+1	Mv	PD
1	814539	307883	679306	1048818	1333611	623887	2.20638
2	506	512	519	526	533	518	1.01367
3	317	321	323	325	327	323	1.00623

Processed Peaks

Peak No	Name	Start RT (mins)	Max RT (mins)	End RT (mins)	Pk Height (mV)	% Height	Area (mV.secs)	% Area
1	Unknown	15.06	16.35	19.96	3179.88	1.62568	354162	4.98549
2	Unknown	26.36	27.47	28.35	176384	90.1747	6.06178e+006	85.3309
3	Unknown	28.35	28.81	29.20	16038.6	8.19962	687911	9.68363

Peak No	Type	St Detect Code	End Detect Code	Is St Mod	Is Max Mod	Is End Mod
1	0	0	0	No	No	No
2	0	0	0	No	No	No
3	0	0	0	No	No	No

No	Start RT (mins)	End RT (mins)	Start Height	End Height	Is St Mod	Is End Mod
1	15.06	19.96	-126.53	93.94	No	No
2	26.36	28.35	-82.43	10.55	No	No
3	28.35	29.20	10.55	49.84	No	No

Polynomial Order	Coeff a	Coeff bx	Coeff cx^2	Coeff dx^3	Coeff ex^4	Coeff fx^5
3	17.4287	-1.01616	0.0214014	-0.000142783	0	0

Figure 7. Gel permeation chromatography test data

In addition, the amphiphilic nature of polymers can be explained by the polymer's ability to emulsify. Conventional water-soluble polymers exhibit hydrophilicity and no lipophilicity, so they do not have emulsifying ability. In contrast, the polymers we obtain by copolymerizing hydrophilic and hydrophobic monomers possess hydrophilicity and lipophilicity and exhibit surfactant properties. The emulsification

of oil and water, as well as the reduction of oil-water interfacial tension, can be achieved. These results can be obtained in the contents of sections 3.3 and 3.4 of the manuscript.

Issue 4: Paragraph 2.4 The method for the measurement of viscosity must be better reported. Which concentrations were tested? Why 7.34 s^{-1}? Was viscosity measured only at one shear rate values or in a range of shear rates and stresses?

Discussion: We apologize for the lack of detail in testing methods. We added a description of the viscosity test method. The modified results are as follows.

The viscosity of the polymer solution to crude oil was determined using a HAAKE MARS III rheometer (Thermo Fischer Electron Co., Germany). The CC24Ti tumbler measuring system was selected for viscosity determination in a CR test mode during viscosity tests. The sample was sheared at 7.34 s^{-1} for 300 s at 50 °C, and the measurements were taken every 30 s. The viscosity-temperature curve was determined in a CR test mode at a shear rate of 7.34 $s^{-1,}$ with recordings made from 20 to 100 °C at a step of 3 °C per 60 s for a total test time of 1600 s.

In addition, we chose the shear rate of 7.34 s^{-1} based on part 6.5.1.4 of the Chinese petroleum industry standard 《SY 5862-2008 Technical Requirements for Polymers for Oil Repellency》, in which a rotational viscometer was used for the determination of the apparent viscosity of polymer solutions with a rotational speed of 6 r/min, which is converted to a shear rate of 7.34 s^{-1}. We have attached a description of the part in Figure 8. and attached the original document of the Chinese standard. In order to ensure the consistency of the results, all of our viscosity measurements were performed at a shear rate of 7.34 s^{-1}.

6.5 表观粘度

6.5.1 Ⅰ型聚丙烯酰胺表观粘度。

6.5.1.1 称取199.00g标准盐水于400mL烧杯中，对粘均相对分子质量2.5×10^7以下Ⅰ型样品采用标准盐水Ⅰ配制溶液，粘均相对分子质量2.5×10^7以上（含2.5×10^7）Ⅰ型样品采用标准盐水Ⅱ配制溶液。准确称取1.0000g试样。调整立式搅拌器的搅拌速度至（400±20）r/min，使标准盐水形成旋涡，在1min内缓慢而均匀地把试样撒入旋涡壁中，继续搅拌2h。

6.5.1.2 称取按6.5.1.1所配溶液20.00g于400mL烧杯中，加标准盐水至100.00g，用磁力搅拌器搅匀。

6.5.1.3 将恒温水浴设定为（45±0.1）℃。

6.5.1.4 UL转子与粘度计连接，将约16mL待测溶液移入测量筒中，恒温10min，然后设定转速为6r/min（7.34s^{-1}），进行表观粘度测定。每个样品测定三次，测试值保留小数点后一位有效数字，取平均值为测定结果。

6.5.2 Ⅱ型聚丙烯酰胺表观粘度。

6.5.2.1 称取（1/S）g样品，精确至0.0001g。称取（200－1/S）g标准盐水Ⅲ于500mL烧杯中，开动恒速搅拌器在（400±20）r/min下沿旋涡壁30s内慢慢加入试样，然后在搅拌速率为（700±20）r/min下搅拌1h。放置24h后，用玻璃棒稍微搅拌再进行稀释。

6.5.2.2 取15.00g按6.5.2.1配制的聚丙烯酰胺母液加入100mL烧杯中，加入35.00g标准盐水Ⅲ，在磁力搅拌器上以（300±20）r/min的转速搅拌15min，得到质量分数0.15%的待测溶液。

6.5.2.3 将恒温水浴设定为（75±0.1）℃，按6.5.1.4测定表观粘度。

Figure 8. Method for determining the apparent viscosity of flooding polymers

Issue 5: Paragraph 2.6 How many times the bottle was inverted?

Discussion: We apologize for the lack of detail in testing methods. In section 2.6, the spontaneous emulsification ability of polymer is evaluated by the inverted bottle method, the fewer the number of times of inversion, the stronger the emulsification ability of polymer, according to the experimental results of 3.3.1, the polymer has a better emulsification effect on heavy oils after inverting the bottle for 50 times. We supplement the experimental description in Section 2.8. The modified results are as follows.

For emulsification analysis, a 30 mL glass bottle was used, combining 4.5 mL of 5000 mg/L polymer solution and 10.5 mL of heavy oil, resulting in an oil-water ratio of 7:3. The bottle was inverted 50 times, and the color of the solution was observed. A uniform black solution after inversion indicated successful emulsification of heavy oil and the polymer.

Issue 6: Paragraph 2.8 Which magnification was used for microscope images?

Discussion: We apologize for the lack of detail in testing methods. In section 2.6, When observing with a microscope, we choose an objective lens with a magnification of 10x and an eyepiece with a magnification of 10x, so the magnification of the microscope observation is 100x. We supplement the experimental description in Section 2.8. The modified results are as follows.

For the examination of the emulsion formed by heavy oil and the polymer solution after emulsification, a small amount was drawn using a pipette and placed onto a microscope slide. A cover slip was carefully placed over the droplet using tweezers. The sample was then positioned on the stage of a Zeiss Primo Star microscope for emulsion image observation with a magnification of 100x.

Issue 7: Paragraph 2.9 Which concentrations were tested? More information on the method should be provided.

Discussion: We apologize for the lack of experimental details. In the test of interfacial tension in part 2.9, we tested the interfacial tension between thick oil and polymer solution, and the concentration of polymer solution includes 1000mg/L, 3000mg/L, 5000mg/L, 7000mg/L, and 10,000mg/L. We added the details of the test. The SVT20N video rotary drop tensiometer is shown in Fig. 9, and the one labeled 1 in the figure is the constant temperature water bath heating unit, labeled 2 is the testing unit, and labeled 3 is the data acquisition unit. Figure 10 shows the glass capillary tube containing the polymer solution

and oil droplets during the test. The test procedure is as follows: (1) open the thermostatic water bath device and adjust the temperature to 50°C. (2) Turn on the interfacial tension test device and preheat for 30 minutes. (3) Load the polymer solution into the glass capillary tube, remove air bubbles and inject a drop of oil using a microinjector. Place the glass capillary tube into the test device. (4) Open the test software in the data acquisition device, set the test parameters and collect the test data. The test temperature is 50°C and the rotational speed is 6000 r/min.

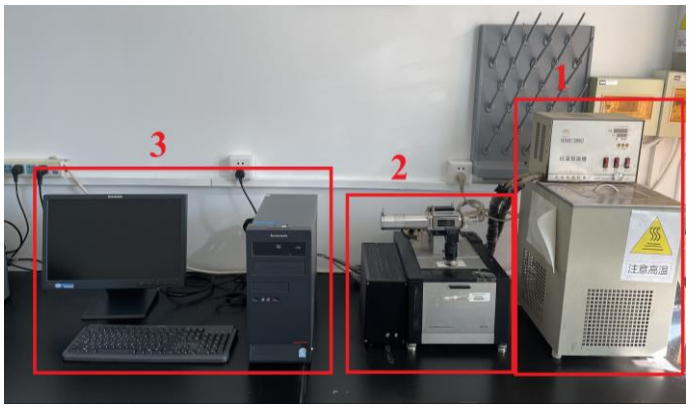


Figure 9. SVT20N video spinning drop tensiometer



Figure 10. Glass capillary tube

Issue 8: Paragraph 2.10 What core slices are? How the contact angle was measured?

Discussion: We apologize for the unclear presentation. Core slices are thin slices of long core cut using a cutter, and the long core and the cut core slices are shown in Figure 11. The SDC200 contact angle meter includes a data acquisition device and a testing device, as shown in Figure 12. The test steps for contact angle are: (1) Turn on the instrument power and start the test software. (2) Place the sample (core slice) on the sample stage. (3) Perform the drop and catch, the volume of the drop is 2 μL, the platform moves from bottom to top, and after contacting the drop, pull back in the opposite direction until the drop is separated from the needle. (4) The software calculates the contact angle and generates a report.



Figure 11. Artificial long core (left) and core slice (right)

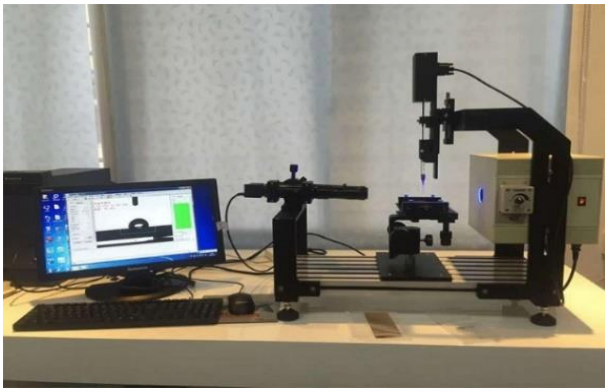


Figure 12. SDC200 contact angle meter

Issue 9: Paragraph 3.1 The FT-IR spectrum of the monomer and physical mixture of the monomers should be provided to draw any conclusions about the peak shift. Integration of the NMR signals should be provided to assess the formation of the polymer.

Discussion: We appreciate this comment. We redrew the FT-IR spectra of part 3.1 with the NMR hydrogen spectra as shown in Figure13. The FT-IR spectra of the monomers were added to the FT-IR spectra, and the integral information of the resonance signals was added to the NMR spectra to evaluate the structure of the polymers. The modified results are discussed as follows.

Figure 13(a) shows the infrared spectra of the monomer and polymer. The spectrum of acrylamide has distinct stretching vibrational bands of amino ($-NH_2$) at 3170 cm^{-1} and 3340 cm^{-1}. This peak slows down and shifts in the polymer spectrum, appearing at 3215 cm^{-1} and 3331 cm^{-1}. The peaks at 1075 cm^{-1} and 1232 cm^{-1} in the infrared spectra of 2-acrylamido-2-methylpropansufonic acid are attributed to the symmetric and asymmetric vibrational absorption peaks of the sulfonic acid group ($-SO_3^-$); this absorption peak in the polymer spectrum is displaced and appears at 1037 cm^{-1} and 1157 cm^{-1}. The peaks at 2853 cm^{-1} and 2922 cm^{-1} in the spectrum of lauryl acrylate are the stretching vibrational bands of methylene ($-CH_2$) and methyl ($-CH_3$) groups, and this peak can also be observed in the polymer spectrum.

The peaks at 3067 cm^{-1} and 3081 cm^{-1} in the spectrum of benzyl acrylate are the characteristic group frequencies of the hydrocarbon bond (C-H) stretching vibration of the benzene ring, and the peaks at 696 cm^{-1} and 737 cm^{-1} are the characteristic absorption peaks of the monosubstituted benzene ring. In addition, absorption peaks of carbonyl group (C=O) were observed at 1773 cm^{-1} and 1671 cm^{-1}. Conclusively, the polymers' spectra contain each reacting monomer's characteristic peaks, proving that we successfully prepared the copolymer PAALB by monomer copolymerization.

To further confirm the molecular structure of PAALB, proton nuclear magnetic resonance spectroscopy was conducted, as displayed in Figure 13(b). The observed peaks and their respective assignments are as follows: the peak at 1.46 ppm corresponds to the H of the methylene ($-CH_2$) on the long chain of lauryl acrylate. The peak at 1.49 ppm corresponds to the H of the methyl ($-CH_3$) on AMPS. The peak at 1.73 ppm corresponds to the H of the secondary methyl on the polymer main chain. The peak at 2.19 ppm corresponds to the H of the methine on the polymer main chain. The peak at 3.41 ppm corresponds to the H of the methylene connected to S on AMPS. The peak near 5.67 ppm corresponds to the H of the methine connected to the benzene ring on benzyl acrylate. The peak near 6.11 ppm corresponds to the H of the amino group ($-NH_2$) on acrylamide. The peak at 7.45 ppm corresponds to the H of the benzene ring on benzyl acrylate. The results obtained from IR and ^{1}H-NMR confirm the successful synthesis of the intended product.

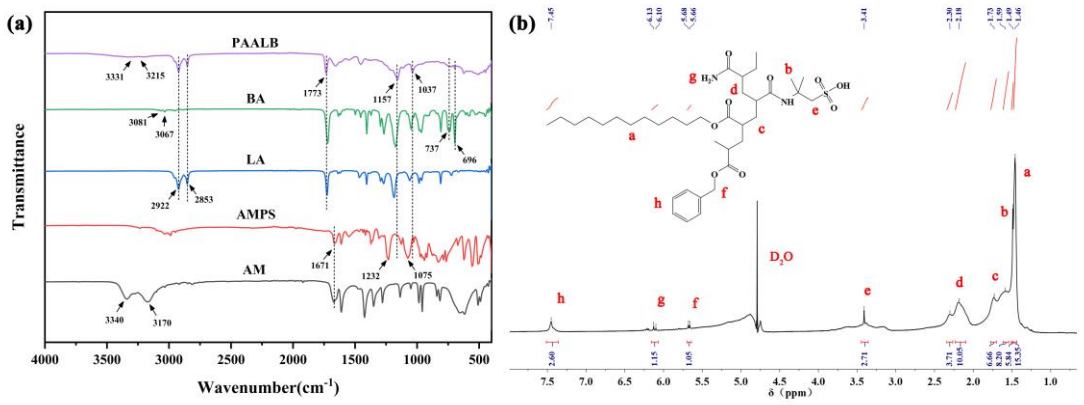


Figure 13. Structural characterization of polymer (a) FT-IR; (b) ^{1}H-NMR

Issue 10: Paragraph 3.2 In the method section should be provided how the CAC concentrations were determined and which method used for the fitting of the data.

Discussion: We appreciate this comment. In part 3.2, due to the hydrophobic association of the polymer, the viscosity of the polymer solution grows at a small rate with increasing concentration at low concentration, and this growth rate increases rapidly when the critical association concentration (CAC) is exceeded. We expanded the concentration range of polymer solution, added 100mg/L, 300mg/L, 500mg/L and 700mg/L concentration data on the basis of the original data, and redrew the viscosity and concentration curves of polymer solution, and used the linear fitting method of Origin software to fit the data at different growth rates. CAC is the turning point of the rate of change of viscosity of the polymer solution, so we take the concentration corresponding to the intersection of the two fitted line segments as the CAC of the polymer. The result is shown in Figure 14. As shown in Figure 14, the CAC of the polymer is 3400 mg/L in deionized water and 4300 mg/L in brine water.

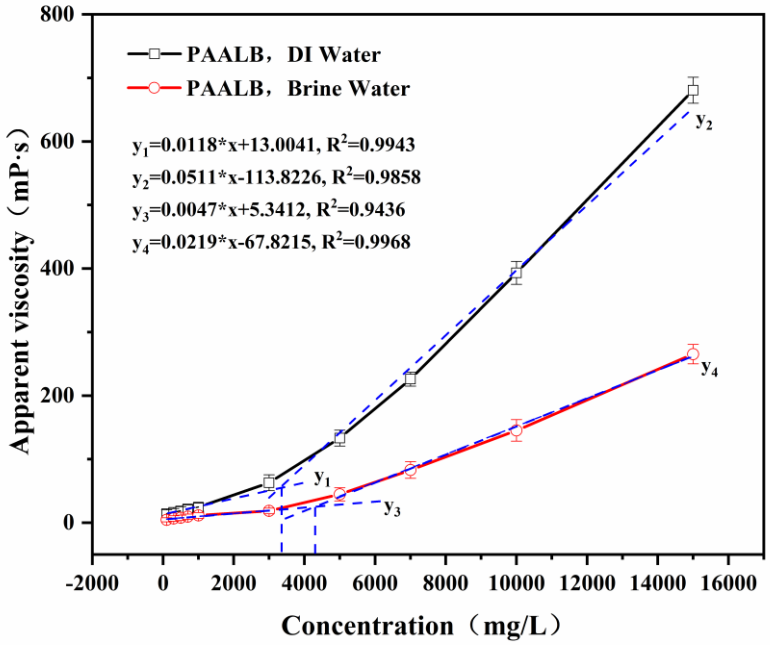


Figure 14. Polymer viscosity curve with concentration

Issue 11: It is unusual that the CAC of the polymers in brine is higher than in water. The authors provided a possible explanation but possibly some references to support this should be added, since generally salts have a different effect on the amphiphiles behaviour.

Discussion: We appreciate this comment. We reviewed the literature and most of the literature only reported critical association concentration (CAC) data for a particular amphiphilic polymer and did not report the effect of salt ions on CAC. We found two papers on the effect of salt ions on the critical association concentration of amphiphilic polymers. They are article number 1:《Influences of structure

and multi-intermolecular forces on rheological and oil displacement properties of polymer solutions in the presence of Ca^{2+}/Mg^{2+} (DOI:10.1039/c6ra25132c)》 and article number 2: 《Preparation and evaluation of fluorinated hydrophobically associating polyacrylamide (DOI: 10.1007/s10965-016-1067-5)》. These two papers concluded that the enhanced polarity and electrostatic shielding in saline solutions lead to the easier aggregation of hydrophobic groups in saline solutions, arguing that typically CAC values are lower in saline water. However, the measurement of CAC in article numbered 1 is based on the increasing trend of the polymer viscosity curve only, and linear fitting and specific fluorescence spectroscopy were not used, so we consider it to be less informative. Article numbered 2 also did not use linear fitting and specific fluorescence spectroscopy to determine the CAC of polymers in brine, and the results of fitting the test data may be in error from their descriptions. We believe that the CAC data obtained by pyrene fluorescence spectroscopy method is the result of the fact that the molar ratio of hydrophobic monomers in the amphiphilic polymers in these other two papers is very small (not more than 1%), while the molar ratio of hydrophobic monomers in the amphiphilic polymers synthesized by us is 20%, so we think it is very likely that the salt ions affect the two polymers in different ways.

We observed the microstructure of the polymer using a scanning electron microscope. The different behavior of the amphiphilic polymer PAALB in deionized water and brine was further explained by analyzing the microstructure of the polymer, and the results are shown in Figures 15 and Figures 16. Figure 15 shows the microstructure of the polymers with different concentrations in deionized water, and it can be observed that the polymers are irregular linear structures at low concentrations (1000 mg/L). As the concentration gradually increased, the linear structure began to interweave and formed a network-like structure (more than 3000 mg/L). As the concentration continued to increase, the network structures gradually intertwined to form lamellar structures (10,000 mg/L), and these lamellar structures piled up layer by layer. It is believed that the formation of linearly interwoven network structures and lamellar structures is due to the binding of hydrophobic groups in the amphiphilic polymer. The formation of these structures increases the volume of the polymer and increases the viscosity of the polymer solution. Therefore, when dense network and lamellar structures are present in the polymer structure, we believe that relatively strong hydrophobic association has occurred in the polymer. Combining the CAC data obtained by pyrene fluorescence spectroscopy and linear fitting methods, we concluded that the CAC of the polymer in deionized water was 3000 mg/L.

Figure 16 shows the microstructures of different concentrations of polymer in brine water. According to Figure 16, it can be seen that the sparse network structure was observed when the polymer solution concentration was below 4000 mg/L, and when the polymer solution concentration was higher than 5000 mg/L, the dense network structure with lamellar stacking structure appeared. When the polymer solution concentration reaches 10000 mg/L, lamellar structure is observed. Therefore, based on the polymer microstructure changes, combined with the CAC data obtained by pyrene fluorescence spectroscopy and linear fitting methods, we believe that the CAC of the polymer in brine is about 5000 mg/L. Based on the results of pyrene fluorescence spectra, linear fitting and microstructure changes, we believe that the CAC of the polymer in brine water is higher than deionized water for the amphiphilic polymer in the manuscript.

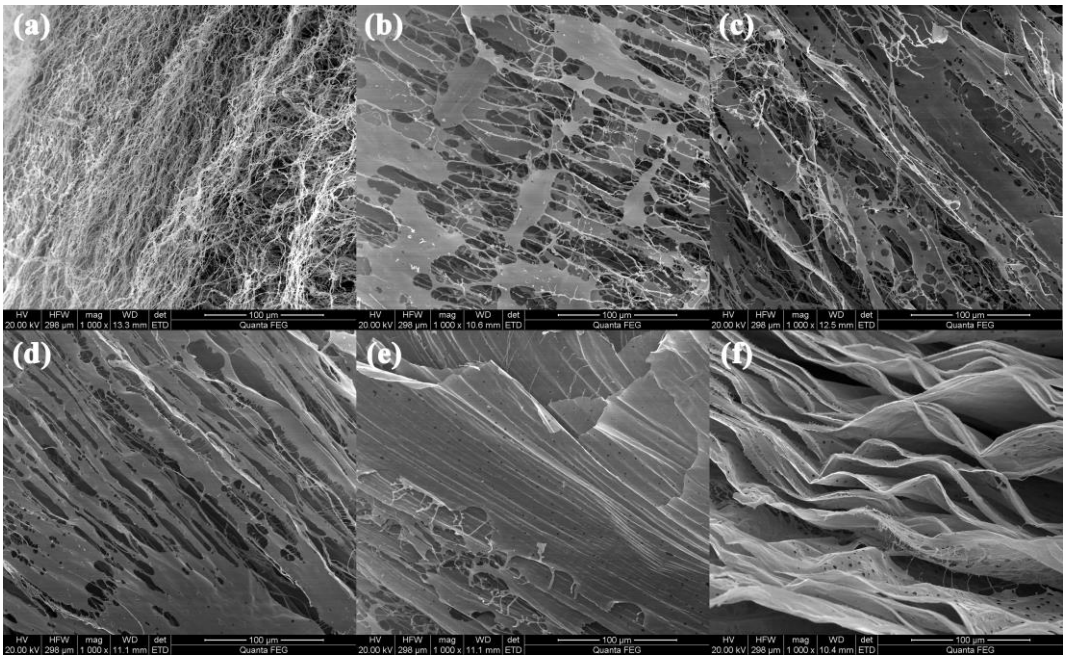


Figure 15. Microstructure of polymer solutions with different concentrations in deionized water. (a. 1000 mg/L; b. 3000 mg/L; c. 5000 mg/L; d. 7000 mg/L; e. 10000 mg/L; f. side view of 10000 mg/L)

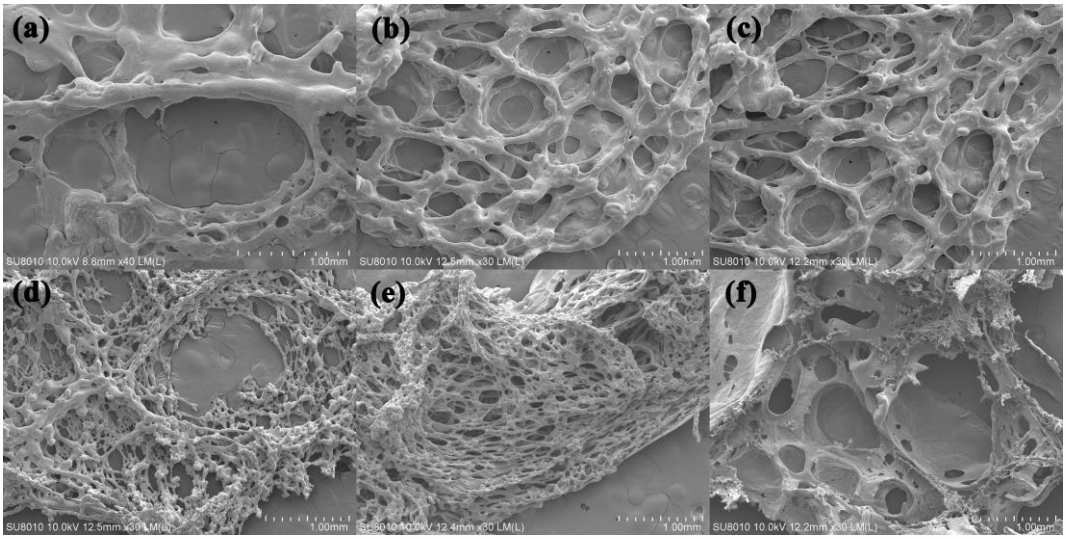
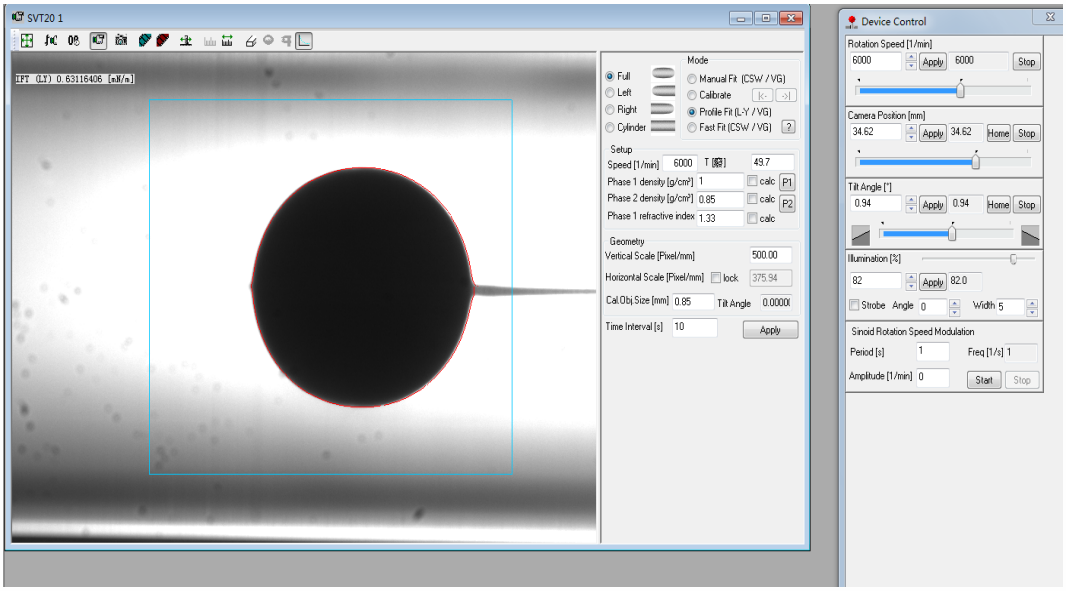
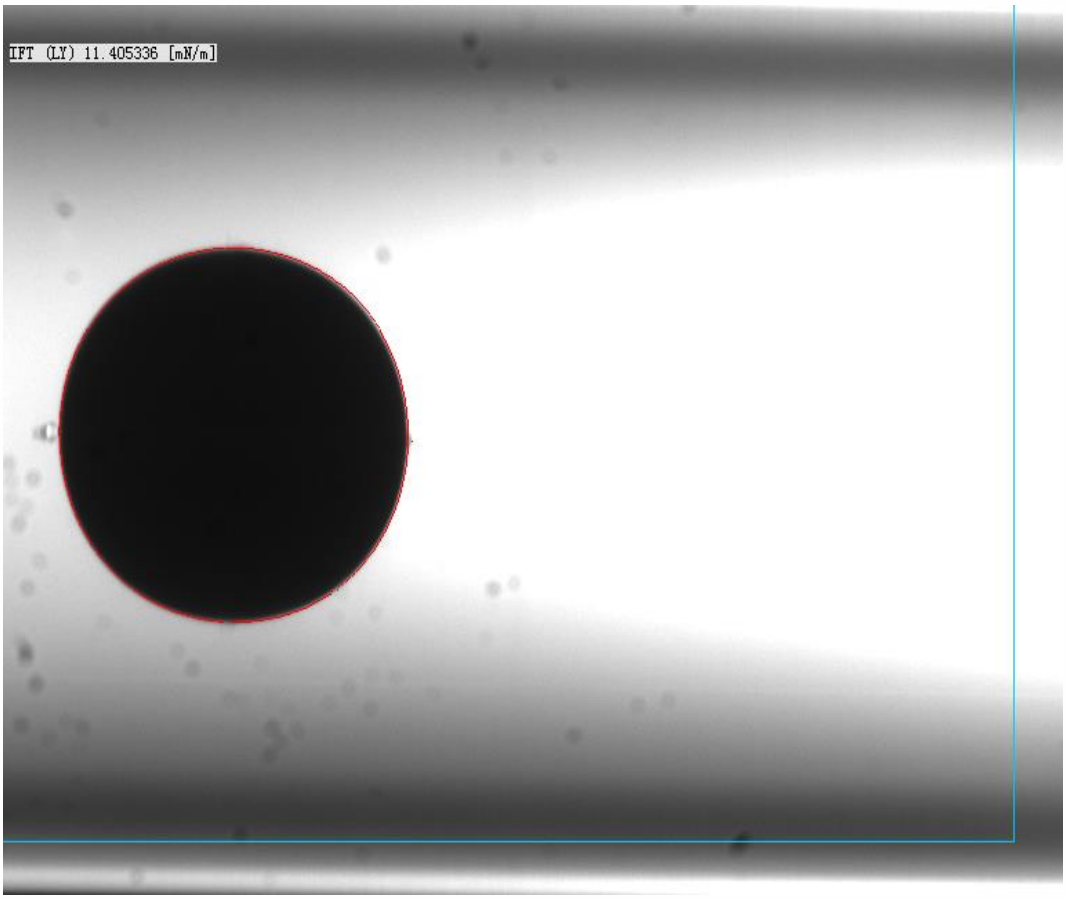


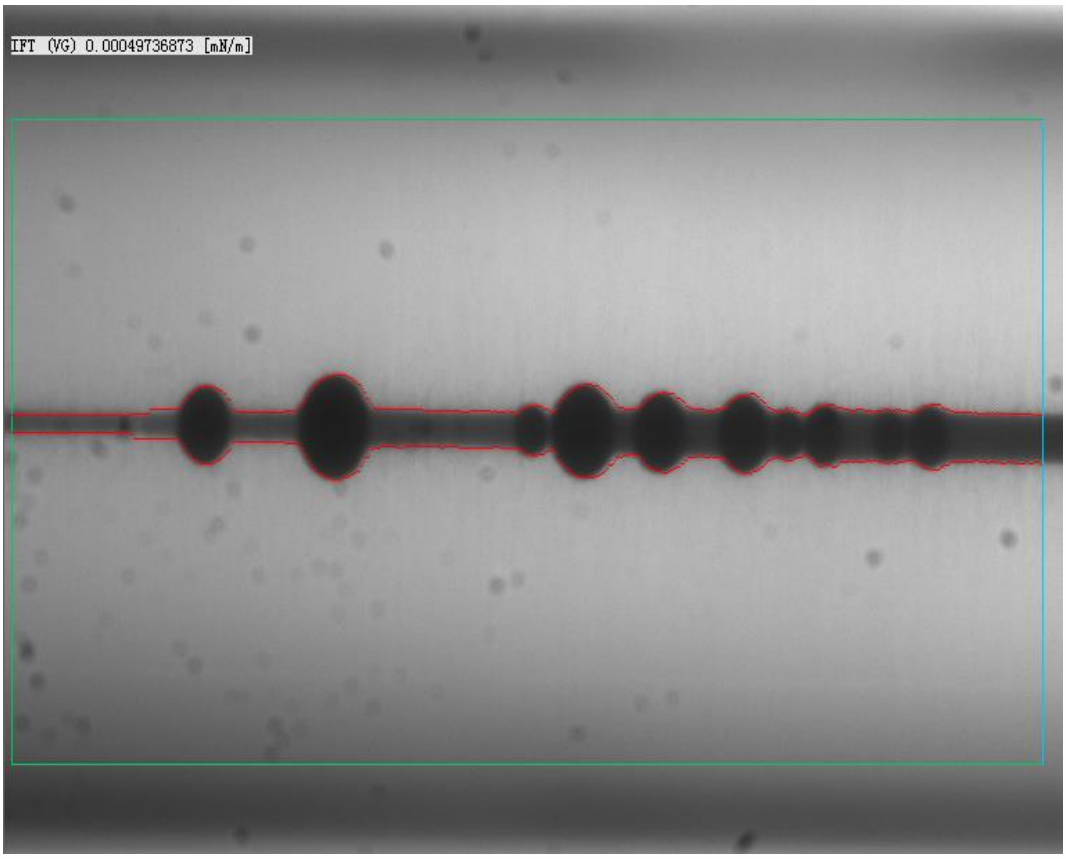
Figure 16. Microstructure of polymer solutions with different concentrations in brine water. (a. 1000 mg/L; b. 3000 mg/L; c. 4000 mg/L; d. 5000 mg/L; e. 7000 mg/L; f. 10000 mg/L)

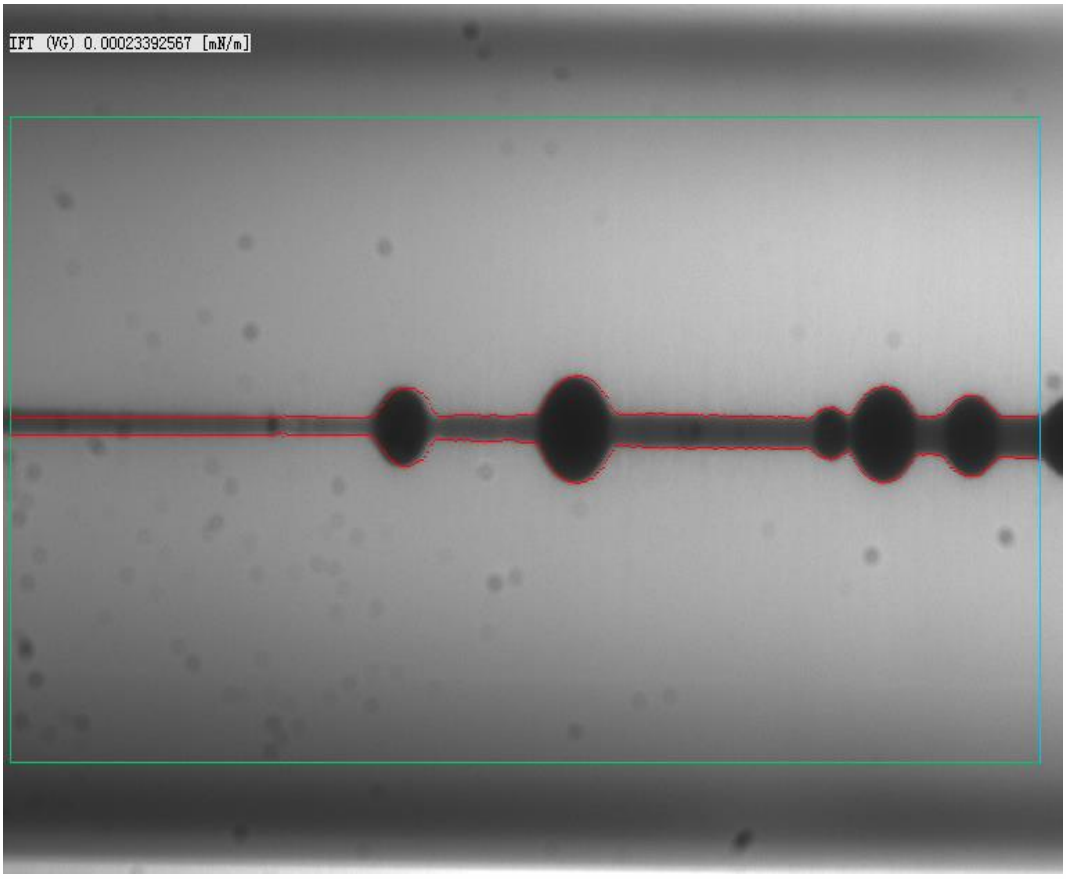
Issue 12: Paragraph 3.2.2 The measured interfacial values are very low between water and the oil without the polymers and very very low with the polymer. Can be they reliably measured using the reported instrument (spinning drop tensiometer)?

Discussion: We appreciate this comment. We used SVT20N video spinning drop tensiometer to measure the interfacial tension between oil and water. The measuring range of this instrument is 1×10^{-6}~2×10^{3} mN/m. Our experimental results are within the measuring range of the instrument. Also in the article 《Evaluation of Interfacial Tension Between Zahra Oil and ASP Solution (DOI: 10.1080/10916466.2015.1039649)》, 《Study of Interfacial Dilational Properties by the Spinning Drop Technique (DOI: 10.3866/PKU.WHXB20090108)》, and 《Interfacial Tension and Foaming Properties of APG and LC Aqueous Solutions with High Salinity in High Temperature (DOI: 1007-2861(2013)19:4<437:GWGYTJ>2.0.TX; 2-V)》, these authors also chose SVT20N video spinning drop tensiometer for interfacial tension measurement, and obtained ultra-low interfacial tension data. Therefore, we believe that the interfacial tension data measured by this instrument is reliable. Finally, we attach the data from the test, as shown in Figure 15. When the interfacial tension is high, in the rotating state, the oil droplets appear spherical in the water phase. When the interfacial tension is low, the globular oil droplets are gradually stretched into bands.


SVT20 1
IFT (LY) 0.63116406 [mN/m]
Mode
Full
Left
Right
Cylinder
Manual Fit (CSW / VG)
Calibrate
Profile Fit (L-Y / VG)
Fast Fit (CSW / VG)
Setup
Speed [1/min] 6000
Phase 1 density [g/cm³] 1
Phase 2 density [g/cm³] 0.85
Phase 1 refractive index 1.33
Geometry
Vertical Scale [Pixel/mm] 500.00
Horizontal Scale [Pixel/mm] 375.94
Cal.Obj.Size [mm] 0.85
Tilt Angle 0.0000
Time Interval [s] 10
Apply
Device Control
Rotation Speed [1/min]
6000 Apply 6000 Stop
Camera Position [mm]
34.62 Apply 34.62 Home Stop
Tilt Angle [°]
0.94 Apply 0.94 Home Stop
Illumination [%]
82 Apply 82.0
Strobe Angle 0 Width 5
Sinoid Rotation Speed Modulation
Period [s] 1 Freq [1/s] 1
Amplitude [1/min] 0 Start Stop


IFT (LY) 11.405336 [mN/m]


IFT (VG) 0.00049736873 [mN/m]


IFT (VG) 0.00023392567 [mN/m]